DEVELOPMENT OF AN INKJET CALIBRATION PHANTOM FOR X-RAY IMAGING STUDIES

Tihomir Georgiev[1], Iliyan Kolev[2], Nikolay Dukov[1], Stanislava Mavrodinova[3], Mariana Yordanova[3], Kristina Bliznakova[1]

[1]Department of Medical Equipment, Electronic and Information Technologies in Healthcare, Faculty of Public Health, Medical University of Varna
[2]Department of Pharmaceutical Chemistry, Faculty of Pharmacy, Medical University of Varna
[3]Training Sector of X-ray Laboratory Assistant, Medical College, Medical University of Varna

ABSTRACT

INTRODUCTION: 3D anthropomorphic models of human tissues have become a requirement for conducting realistic virtual studies. One of the current directions in the research of X-ray imaging is the development of physical models with 3D printing techniques using specific materials aiming to obtain replica of the human body tissues with similar radiological characteristics.

Aim: The aim of this study is to create a calibration phantom for establishing the X-ray properties of different cartridge infills and their suitability to represent the X-ray properties of different breast types.

MATERIALS AND METHODS: A physical calibration model consisting of 22 objects was designed and printed by using an inkjet printer. A mixture was obtained from 5 mL printer ink and 3 g of potassium iodide (KI), which was used to fill the printer's cartridge and to print the model on a set of plain office paper. Experimental X-ray images of the physical model were acquired on radiographic system SEDECAL X PLUS LP+. The obtained attenuation coefficient of the printing mixture was evaluated and compared to the breast tissue coefficients corresponding to the used X-ray energy.

RESULTS AND DISCUSSION: The physical model was printed on ten office sheets and stacked above one another. The obtained attenuation coefficient of the printing mixture was found very similar to that of the glandular tissue of the breast for the used X-ray energy.

CONCLUSION: The obtained printer ink-KI mixture is suitable for representing the glandular part of breast tissue. The method has the potential to be used for creation of a realistic physical breast model.

Keywords: *3D physical breast models, low-cost printing, inkjet printing*

Address for correspondence:
Tihomir Georgiev
Faculty of Public Health
Medical University of Varna
55 Marin Drinov St
9002 Varna
e-mail: T.Georgiev@mu-varna.bg

Received: February 18, 2021
Accepted: March 7, 2021

INTRODUCTION

Three-dimensional (3D) anthropomorphic models of human tissues have become a requirement for conducting realistic virtual studies. Anthropomorphic phantoms are used to assess medical equipment, technology efficiency, as well as new algorithms for image reconstruction (1,2). The approaches to create anthropomorphic models of human tissues depend on whether this model is com-

putational or physical. In the latter case, there are several approaches, which include casting (3) or 3D printing. Among the 3D printing techniques are the fuse-deposition technology (FDM), stereolithography (STL), and jetting technology (4,5). In recent years, researchers have proposed the use of popular inkjet printers as a suitable solution in the development of a low-cost radiography phantom (6–10). Sikaria *et al.* (6) used 3D printing with two-dimensional (2D) paper lesions inserts to create a physical model of a breast—3D printing with polymer material with added TiO_2 and 2D paper prints with iopamidol for lesion inserts. The advantage of the model is the easiness to produce it. Amongst the limitations of their approach are the higher cost as well as the need of adding tungsten or copper to the TiO_2 concentration in order to achieve higher attenuation material. Another method is the use of potassium iodide (KI). A phantom of the abdomen (7) was created based on patient CT image with KI. For this purpose, two sets of twelve square objects were printed and used in a calibration method to correct the model printing. The printed slices were then stacked together to form a complete 3D phantom, imaged at CT facilities and consequently evaluated. Recently, a liver phantom was created by Pegues *et al.* (10), who used two types of ink to print the liver tissue. Specifically, sodium bromide (NaBr) was used to print the unenhanced tissue, while KI was used for the enhanced tissue. Results for NaBr showed linearity between the infill percentage, in the range of 50% to 100%, and the attenuation coefficient. The authors created a colormap of the 3D liver model to be suitable for their printer. Once this was done, linearity evaluation and phantom printing were both easily performed.

Further, Ikejimba *et al.* reported on the creation of physical breast phantoms based on inkjet technology. The authors used a computational breast phantom as a source for the physical breast model, which was printed slice by slice with an inkjet printer with cartridges filled with a mixture of iohexol and printer ink to represent the glandular tissue. Several types of parchment paper were evaluated for their suitability to mimic the X-ray properties of the adipose tissue in the diagnostic X-ray range (8). Results showed that printer ink with added iodine can be used to mimic glandular tissue, while parchment paper can be used to mimic adipose tissue. Another similar experiment was reported by Makeev *et al.* (9) with iohexol added to the ink and printed on a baking paper. along with added microcalcifications, in order to compare two full-field digital mammography (FFDM) detectors.

AIM

The purpose of this study is to create a calibration phantom for establishing the X-ray properties of different cartridge infills and their suitability to represent the X-ray properties of different breast types.

MATERIALS AND METHODS

Phantom Design

To create the modified ink, KI was mixed with the printer ink as follows: 3 g of KI were mixed in 5 mL of compatible black ink—InkTec refill ink, for about 10 minutes at room temperature. The mixture was injected into an empty rechargeable cartridge for commercially available inkjet printer HP deskjet 1050A.

A pattern with 22 squares 20 mm x 20 mm was created in Microsoft Word (Fig. 1). There were 12 different black cartridge infills—from 0% (no ink) to 100% (full ink). The infills were distributed equally with infill increase step of 9.09%.

Then 10 sheets of paper were printed with the created pattern and stacked together. The used paper was 80 g/m^2 plain printer paper. The thickness of one sheet of paper was measured at 0.1 mm. There was no ink deposition on each square 1, which was with infill 0%, therefore 11 squares per set were printed with the modified ink. The squares in the first and second row were positioned in a decreasing infill order from 100% to 0%, while the squares in the third and fourth rows were randomly placed.

Experimental Work

X-ray images of the produced pattern were acquired at St. Anna Hospital in Varna, Department of Image Diagnostics, using radiographic system SEDECAL X PLUS LP+ with anode voltage 45 kVp and current 125 mA. In addition, X-ray images of 10 stacked blank paper sheets were acquired. The images were processed with the image processing program ImageJ (19).

Phantom Characterization

Phantom characterization was obtained by plotting the measured attenuation coefficient as a

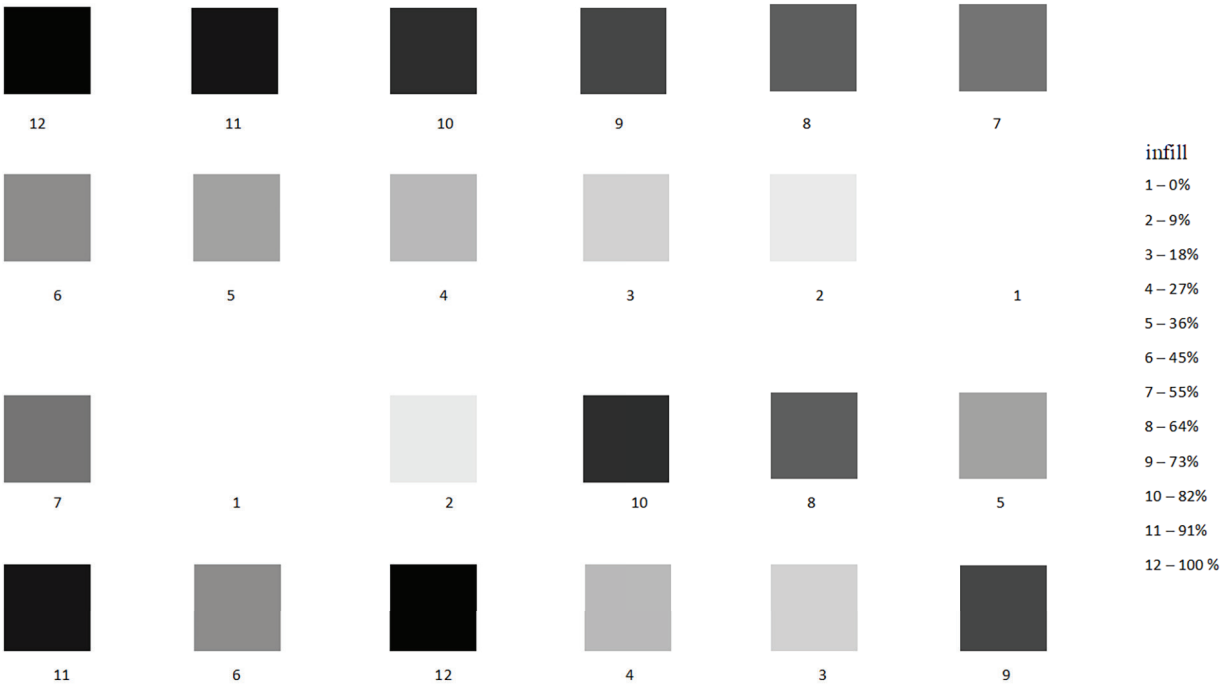

Fig. 1. A screenshot of the developed pattern in Microsoft Word.

function of the infill. The attenuation coefficient, μ, was calculated from the acquired X-ray image of the phantom (shown in Fig. 2**B**) using the Beer-Lambert law:

$$\mu_i = \ln (I_O/I_{Ii}) \quad (1)$$

where i varies from 1 to 5, I_O is the average intensity value of the two background regions (RoS) positioned to the left and to the right of the square and I_{Ii} is the average intensity value of each of five overlapping regions placed in the central part of the square object (RoI). The linear attenuation coefficient μ_i is the attenuation coefficient in the respective RoI inside the pattern. The RoS were defined with dimensions 10.08 mm x 10.08 mm, while each RoI had dimensions 4.96 mm x 4.96 mm.

Statistical Methods

The statistical methods were mainly explored to obtain the linear attenuation coefficients for the different infill objects: mean value and standard deviation. Mean value for each square was calculated by using equation 1. Further, the value (μ) and the

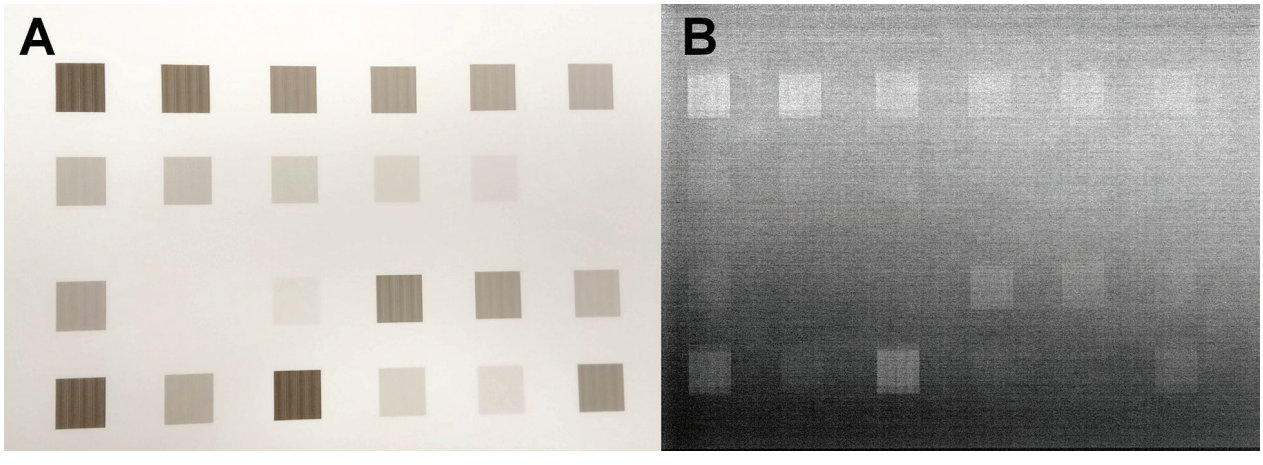

*Fig. 2. Image of the printed physical phantom (**A**) and X-ray image of the phantom (**B**).*

standard deviation (σ) of each pattern was calculated as follows:

$$\mu = (\mu_1 + \mu_2 + \mu_3 + \mu_4 + \mu_5) / 5 \quad (2)$$

$$\sigma = \sqrt{\frac{\Sigma(\mu_i - \mu)^2}{5}} \quad (3)$$

where μ_i is the attenuation coefficient for each of the five RoI of the pattern and μ is the mean value of the attenuation coefficient calculated by using equation 2.

RESULTS

The developed physical calibration phantom is shown in Fig. 2**A**. The placement of the printed squares corresponds to the digital model shown in Fig. 1. The acquired X-ray image of the phantom is shown in Fig. 2**B**, where the brightest squares correspond to a print with infill of 100%.

Fig. 3**A** summarizes the results for the linear attenuation coefficients in cm^{-1} recorded against the infill percentage from the set with the squares placed in the first and second rows of the phantom (squares printed in decreasing order of infill). A linear trend and a second order polynomial are used to fit the obtained results for the linear attenuation coefficient as a function of the object's infill (Fig. 3**A**). The calculated attenuation coefficients of the square objects with infill less than 30% were very similar to each other. This may be due to the high permeability on low iodide concentrations and the fields' non-uniformity details.

Results for the second set of squares—placed in rows 3 and 4 (Figs. 1 and 2**A**), were similar to the first set for the respective infill, except for the ones for 100%, 82%, and below 30%. However, when fitted with second order polynomial, R^2 was 0.901.

Theoretical calculations of the linear attenuation coefficients of glandular, adipose and skin tissues were performed by using the NIST XCOM application program (20) and shown in Fig. 3**B** in comparison to the experimentally derived attenuation coefficient of the mixture. The elemental composition of the glandular and adipose tissues was taken from https://physics.nist.gov/PhysRefData/XrayMassCoef/tab2.html (21), while that for the skin data was adapted from https://van.physics.illinois.edu/qa/listing.php?id=779&t=human-skin (22). The calculated theoretical attenuation coefficient that corresponds to an object printed with 100% infill is 0.418 cm^{-1} which is very close to the calculated glandular tissue attenuation of 0.427 cm^{-1} at this X-ray energy (45kVp). This suggests that the glandular tissue of the breast may be printed with the proposed mixture with a 100% infill. For comparison, the theoretical linear attenuation for the adipose and the skin tissues is 0.347 cm^{-1} and 0.634 cm^{-1}, respectively.

Other research studies related to the use of contrast materials in the production of physical phantoms also have found iodine-based inks suitable to represent human tissue features. Jahnke *et al.* (7) reported linearity between Hounsfield units (HU) and grayscale when using KI solution ink after applying

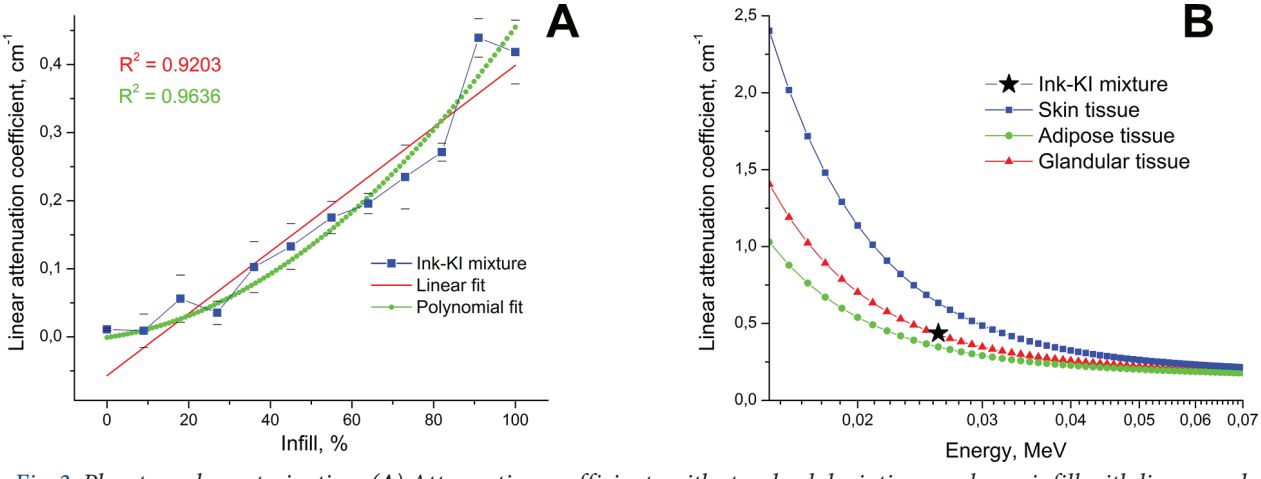

*Fig. 3. Phantom characterization: (**A**) Attenuation coefficients with standard deviation marks vs. infill with linear and second-order polynomial approximation, (**B**) comparison of total attenuation coefficients of glandular, adipose, and skin tissues and the experimental value for the obtained printing mixture at 100% infill.*

a correction formula. Ikejimba *et al.* (8) found that iodine-based contrast agent may be used as ink in certain concentrations. With the prepared mixture they printed a breast physical phantom on a parchment paper. The evaluation showed that iodine may be used to represent the glandular tissue.

There were several limitations of this study related to the nature of the ink, printer, and the X-ray unit itself. Firstly, the KI changes with time and exposure to air. The KI also tended to crystallize inside the cartridge and the cartridge had to be flushed and refilled. Secondly, images were not uniform but rasterized and there were uncertainties whether ink deposited on the paper was strictly the same on each sheet and if there was a strict linear relation between infill setting and actual deposited ink. Similar problems were reported by Pegues *et al.* (10) who used NaBr and KI solutions. Finally, the exposure field was non-uniform resulting in slight deviations in measured values for objects with the same infill.

The efforts of the team are focused on the developing of a complete breast phantom based on iodine contrast material. Based on the results of this study, the complete 3D breast phantom will be printed on a plain office paper. For this purpose, the patient breast data will be segmented into glandular, adipose, and skin tissues. Furthermore, the proposed mixture will be exploited to print the glandular and skin tissue. To complete the validation and evaluation of the physical phantom, experiments on a CT system are planned.

CONCLUSION

This paper presented the first steps in the creation of an anthropomorphic breast phantom based on low-cost inkjet technology. The results of this study indicate that the obtained printer ink-KI mixture is suitable for representing the glandular part of the breast tissue for the diagnostic X-ray energy range. The established method will be used for the creation of a realistic physical breast model.

Acknowledgements:

This research is supported by the Bulgarian National Science Fund under grant agreement DN17/2.

REFERENCES

1. Bliznakova K, Buliev I, Bliznakov Z. Anthropomorphic phantoms in image quality and patient dose optimization. A EUTEMPE Network book. IOP Publishing; 2018.
2. Zaidi H, Tsui BMW. Review of computational anthropomorphic anatomical and physiological models. Proc IEEE. 2009; 97(12):1938-53. doi:10.1109/JPROC.2009.2032852.
3. Leithner R, Knogler T, Homolka P. Development and production of a prototype iodine contrast phantom for CEDEM. Phys Med Biol. 2013;58(3):N25-35. doi: 10.1088/0031-9155/58/3/N25.
4. Carton AK, Bakic P, Ullberg C, Derand H, Maidment AD. Development of a physical 3D anthropomorphic breast phantom. Med Phys. 2011;38(2):891-6. doi: 10.1118/1.3533896.
5. Clark M, Ghammraoui B, Badal A. Reproducing 2D Breast Mammography Images with 3D Printed Phantoms. Proc SPIE. 2016; 9783:97830B. doi:10.1117/12.2217215.
6. Sikaria D, Musinsky S, Sturgeon GM, Solomon J, Diao A, Gehm ME, et al. Second generation anthropomorphic physical phantom for mammography and DBT: Incorporating voxelized 3D printing and inkjet printing of iodinated lesion inserts. Proc SPIE. 2016; 9783:978360-1. doi:10.1117/12.2217667.
7. Jahnke P, Limberg FR, Gerbl A, Ardila Pardo GL, Braun VP, Hamm B, et al. Radiopaque Three-dimensional printing: A method to create realistic ct phantoms. Radiology. 2017;282(2):569-75. doi: 10.1148/radiol.2016152710.
8. Ikejimba LC, Graff CG, Rosenthal S, Badal A, Ghammraoui B, Lo JY, et al. A novel physical anthropomorphic breast phantom for 2D and 3D x-ray imaging. Med Phys. 2017;44(2):407-16. doi: 10.1002/mp.12062.
9. Makeev A, Ikejimba LC, Salad J, Glick SJ. Objective assessment of task performance: a comparison of two FFDM detectors using an anthropomorphic breast phantom. J Med Imaging (Bellingham). 2019;6(4):043503. doi: 10.1117/1.JMI.6.4.043503.
10. Pegues H, Knudsen J, Tong H, Gehm ME, Wiley BJ, Samei E, et al. Using inkjet 3D printing to create contrast-enhances textures physical phantoms for CT. Proc SPIE, 2019; 10948. doi: 10.1117/12.2512890.

11. Ivanov D, Bliznakova K, Buliev I, Popov P, Mettivier G, Russo P, et al. Suitability of low density materials for 3D printing of physical breast phantoms. Phys Med Biol. 2018 Sep 6;63(17):175020. doi: 10.1088/1361-6560/aad315.

12. Dukov N, Bliznakova K, Teneva T, Marinov S, Bakic P, Bosmans H, et al. (2021) Experimental evaluation of physical breast phantoms for 2D and 3D breast x-ray imaging techniques. IFMBE Proc. 2021; 80:544-52.

13. Bliznakova K. The advent of anthropomorphic three-dimensional breast phantoms for X-ray imaging. Phys Med. 2020;79:145-61. doi: 10.1016/j.ejmp.2020.11.025.

14. di Franco F, Sarno A, Mettivier G, Hernandez AM, Bliznakova K, Boone JM, et al. GEANT4 Monte Carlo simulations for virtual clinical trials in breast X-ray imaging: Proof of concept. Phys Med. 2020;74:133-42. doi: 10.1016/j.ejmp.2020.05.007.

15. Feradov F, Marinov S, Bliznakova K. Physical breast phantom dedicated for mammography studies. IFMBE Proc. 2020;76:344-52.

16. Bliznakova K, Mettivier G, Russo P, Bliznakov Z. Validation of a software platform for 2D and 3D phase contrast imaging: Preliminary subjective evaluation. Proc SPIE. 2020; 11513: 1151312. doi: 10.1117/12.2564356.

17. Daskalov S, Okkalidis N, Boone JM, Marinov S, Bliznakov Z, Mettivier G, et al. Anthropomorphic physical breast phantom based on patient breast CT data: Preliminary results. IFMBE Proc. 2020;76:367-74.

18. Mettivier G, Sarno A, Franco FD, Bliznakova K, Bliznakov Z, Hernandez AM, et al. The Napoli-Varna-Davis project for virtual clinical trials in X-ray breast imaging. 2019 IEEE Nuclear Science Symposium and Medical Imaging Conference, NSS/MIC 2019. 2019; art. no. 9059828.

19. https://imagej.net

20. https://physics.nist.gov/PhysRefData/Xcom/html/xcom1.html

21. https://physics.nist.gov/PhysRefData/XrayMassCoef/tab2.html

22. https://van.physics.illinois.edu/qa/listing.php?id=779&t=human-skin